



Reading the Epigenetic Clock: A Comparative Analysis of DNA Methylation Markers for Age Estimation in Semen, Saliva, and Touch DNA

Febria Suryani¹, Bryan Helsey², Leonardo Simanjuntak^{3*}, Karina Chandra⁴, Mustafa Mahmud⁵, Lisha Sandrina⁶, Ahmad Erza⁷

¹Department of Health Sciences, Emerald Medical Center, Jakarta, Indonesia

²Department of Biomolecular Science and Translational Medicine, Quezon Medical Center, Quezon, Philippines

³Department of Obstetrics and Gynecology, CMHC Research Center, Palembang, Indonesia

⁴Department of Anesthesiology and Intensive Care, CMHC Research Center, Palembang, Indonesia

⁵Department of Thoracic Surgery, CMHC Research Center, Palembang, Indonesia

⁶Department of Optometry, CMHC Research Center, Palembang, Indonesia

⁷Department of Criminal Law, Enigma Institute, Palembang, Indonesia

ARTICLE INFO

Keywords:

Age estimation
DNA methylation
Forensic epigenetics
Forensic intelligence
Touch DNA

***Corresponding author:**

Leonardo Simanjuntak

E-mail address:

leo.simanjuntak@cattleyacenter.id

All authors have reviewed and approved the final version of the manuscript.

<https://doi.org/10.59345/sjfm.v3i1.233>

ABSTRACT

Introduction: The capacity to predict an individual's age from biological evidence constitutes a significant advancement in forensic intelligence. DNA methylation, a stable epigenetic mark, provides a molecular basis for "epigenetic clocks." However, the operational reliability of these clocks necessitates rigorous validation across diverse biological samples and populations, particularly for challenging, low-template touch DNA evidence. **Methods:** Following approval from the Ethical Committee of CMHC Indonesia (No. 128/EC/CMHC/2023), we recruited 150 healthy Indonesian male volunteers aged 18-65. Semen, saliva, and high-yield standardized touch DNA samples were collected. DNA was extracted, quantified fluorometrically, and subjected to bisulfite conversion with efficiency controls. The methylation levels of a curated five-CpG panel (ELOVL2, FHL2, TRIM59, KCNQ1DN, C1orf132) were quantified using a rigorously controlled pyrosequencing workflow. Body-fluid-specific age prediction models were developed using multiple linear regression, validated with 10-fold cross-validation, and assessed for statistical assumptions including multicollinearity. **Results:** The models for semen and saliva demonstrated high predictive accuracy, yielding Mean Absolute Deviation (MAD) values of 3.19 years ($R^2=0.94$) and 3.55 years ($R^2=0.92$), respectively. The model developed from high-yield touch DNA was less precise but still highly informative, with a MAD of 5.49 years ($R^2=0.85$). All models satisfied the assumptions of linear regression, with Variance Inflation Factors below 2.5 indicating low multicollinearity. The 95% prediction intervals were narrowest for semen, reflecting its superior precision. **Conclusion:** This study validates a robust, targeted epigenetic panel for age prediction in a Southeast Asian population. We present highly accurate, tissue-specific models for semen and saliva, suitable for immediate consideration in forensic casework. The touch DNA model, while requiring cautious interpretation, provides a valuable framework for generating investigative leads from trace evidence. Our findings underscore the critical importance of tissue-specific modeling and provide a detailed methodological and statistical blueprint for the responsible implementation of forensic age estimation.

1. Introduction

The operational scope of forensic genetics is undergoing a paradigm shift, expanding from its traditional role in identity confirmation to the

generation of actionable investigative intelligence from unknown biological samples.¹ Within this evolving landscape of Forensic DNA Phenotyping (FDP), the ability to accurately predict an individual's

chronological age represents one of the most transformative capabilities for law enforcement and human identification efforts. An age estimate can refine suspect pools, guide investigative direction in "no-suspect" cases, corroborate or refute witness statements, and provide critical information for identifying victims of mass casualty events.² Unlike categorical traits such as eye or hair color, age is a continuous variable, and its prediction requires robust statistical models that can capture the subtle, progressive molecular changes that occur throughout the human lifespan. The search for a reliable molecular chronometer has led researchers through investigations of telomere attrition and somatic rearrangements, yet these have been largely supplanted by the field of epigenetics. DNA methylation, the addition of a methyl group to cytosine bases, has emerged as the foundation of the most promising "epigenetic clocks." This epigenetic modification is biochemically stable in forensic samples and changes in a predictable, systematic manner with age at specific CpG dinucleotides throughout the genome.³ These changes are not merely random decay; they represent a complex interplay between programmed developmental processes and stochastic cellular damage, making the epigenome a living record of an individual's journey through time.⁴

The development of epigenetic clocks has progressed through several generations. Initial landmark studies demonstrated the concept using genome-wide microarrays to build powerful pan-tissue and tissue-specific models, often involving hundreds of CpG sites.⁵ While scientifically groundbreaking, these "first-generation" clocks are ill-suited for routine forensic casework due to high cost, significant DNA input requirements, and complex data analysis. This has driven the field towards the development of targeted assays, which represent a more pragmatic "second-generation" approach. These assays focus on a small, curated panel of the most informative CpG sites, analyzed using sensitive and quantitatively precise techniques like bisulfite pyrosequencing.⁶ This strategy strikes a critical balance, optimizing for predictive accuracy while adhering to the forensic

constraints of limited sample material, degraded DNA, and the need for cost-effective, high-throughput workflows. The selection of markers for such a targeted panel is a crucial design consideration. A robust panel should be built not just on markers with the strongest individual correlation to age, but on a combination that provides a holistic and buffered signal. This study focuses on a curated five-marker panel designed to achieve this balance. The panel is anchored by a CpG site in elongation of very long chain fatty acids 2 (ELOVL2), a locus whose methylation status has an exceptionally strong and widely validated linear correlation with age across numerous tissues and populations.⁷ To complement this primary predictor, we included markers in genes with diverse functions: FHL2 (a signaling adapter), TRIM59 (involved in cell cycle regulation), KCNQ1DN (a potassium channel-related gene), and C1orf132 (a gene of less-defined function). This multi-locus approach is designed to be resilient to anomalous methylation at any single site and to capture a more integrated signal of systemic aging.

Despite promising results in the literature, two significant gaps hinder the widespread, responsible implementation of this technology. The first is the issue of tissue specificity. Most models are developed on blood or saliva, yet casework involves a spectrum of biological materials. Semen, a critical evidence type in sexual assault investigations, has a unique cellular and epigenetic composition.⁸ Touch DNA, the low-template material left on handled objects, represents the ultimate forensic challenge due to its minimal quantity, potential for degradation, and complex cellular makeup. Applying a model built on one tissue to another without rigorous comparative validation is scientifically unsound and risks generating dangerously misleading investigative leads.

The second gap is population-specific validation. Epigenetic patterns, including the rate of epigenetic aging, can be influenced by genetic ancestry and environmental factors.⁹ Validating these tools in diverse global populations is therefore not merely an academic exercise but an ethical and scientific necessity. This is particularly true for the genetically diverse populations of Southeast Asia, for whom

forensic epigenetic data remains sparse. The novelty of this research is threefold. First, it provides a direct, simultaneous, and methodologically rigorous comparison of age prediction accuracy across three forensically vital and biologically distinct matrices: semen, saliva, and high-yield standardized touch DNA. Second, it develops and validates a specific five-marker age prediction tool in a well-characterized cohort of Indonesian males, providing crucial data for this under-represented Southeast Asian population. Third, it moves beyond a simple report of accuracy by incorporating a detailed analysis of the statistical models and a deep, critical discussion of the biological mechanisms and practical implementation challenges.¹⁰ Therefore, the primary aims of this study were To provide a transparent and reproducible methodology for quantifying DNA methylation at five age-associated CpG sites (ELOVL2, FHL2, TRIM59, KCNQ1DN, and C1orf132); To develop and rigorously validate—using cross-validation and assessment of statistical assumptions—three separate, body-fluid-specific age prediction models for semen, saliva, and touch DNA; To critically evaluate and compare the performance of these models, grounding the observed differences in accuracy in the known pathophysiology and unique biological characteristics of each sample type; To establish a foundational framework for the responsible operational implementation of this technology, including a discussion of reporting practices and limitations.

2. Methods

This study was conducted in strict compliance with the principles of the Declaration of Helsinki. The research protocol, including all recruitment, consent, and sampling procedures, was reviewed and approved by the Ethical Committee of CMHC Indonesia (No. 128/EC/CMHC/2023). A cohort of 150 male volunteers was recruited between January and June 2024 from Palembang, South Sumatra, Indonesia. Recruitment occurred through public notices at university campuses and local community centers, representing a convenience sampling strategy. To characterize the cohort and assess potential confounding variables, all participants completed a

detailed, anonymized questionnaire. Data collected included age, self-declared ethnicity (all participants identified as native to South Sumatra), occupation, and key lifestyle factors including smoking status (never-smoker, former smoker, current smoker with pack-years), and weekly alcohol consumption. Exclusion criteria were: age outside the 18-65 year range, a history of cancer or autoimmune disease, current use of medications known to significantly impact DNA methylation, and blood transfusion within the previous six months. All participants provided written informed consent prior to enrollment. Chronological age was verified against a government-issued identification card.

For each volunteer, three biological samples were collected under controlled conditions. Saliva: Participants abstained from eating, drinking, and smoking for 30 minutes, then provided approximately 2 mL of whole saliva via passive drooling into a sterile tube containing 2 mL of a DNA stabilization buffer (DNA Genotek). Samples were inverted to mix and stored at ambient temperature as per the manufacturer's protocol. Semen: Participants were provided with sterile, wide-mouthed polypropylene containers for sample collection via masturbation in a private facility. Samples were processed within one hour of collection. Standardized Touch DNA: To create a standardized substrate for model building, a protocol for generating high-yield touch samples was employed. After washing hands and acclimating for 15 minutes, each volunteer vigorously rubbed a sterile 2.0 mL polypropylene tube between their thumb, index, and middle fingers for a continuous two-minute period. This protocol was designed to deposit sufficient material for robust model training, and it is acknowledged that this does not represent all forensic scenarios, particularly single, brief-touch events. All samples were assigned anonymous identifiers and processed. Aliquots not for immediate use were archived at -80°C. DNA extraction protocols were tailored to each sample type. An extraction blank (containing only reagents) was included with every batch of 12 samples to monitor for reagent and environmental contamination. Saliva: DNA was extracted from a 500 µL aliquot of the stabilized saliva

using the prepIT-L2P purification protocol (DNA Genotek) followed by isopropanol precipitation. Semen: DNA was extracted from a 20 μ L aliquot of whole semen using the QIAamp DNA Investigator Kit (QIAGEN, Hilden, Germany). The protocol included incubation with Proteinase K and a final concentration of 0.8 M Dithiothreitol (DTT) to ensure complete lysis of sperm heads. Touch DNA: Cellular material was recovered from the handled tubes using the double-swab technique. Two sterile cotton swabs were moistened with nuclease-free water, used to swab the entire tube surface, and then co-extracted using the QIAamp DNA Investigator Kit with 1 μ g of carrier RNA added to enhance recovery from the low-template sample.

DNA concentration was quantified using the Qubit 4 Fluorometer with the Qubit dsDNA High Sensitivity Assay Kit (Thermo Fisher Scientific, USA). This fluorometric method was chosen for its accuracy and specificity for double-stranded DNA, which is critical for low-concentration samples. The assay's Limit of Quantification (LOQ) was established at 0.05 ng/ μ L. Purity was assessed using a NanoDrop spectrophotometer to ensure A260/280 ratios were within the 1.8-2.0 range. For each sample, up to 500 ng of DNA (or the entire eluate for touch samples with <500 ng total yield) was subjected to bisulfite conversion using the EZ DNA Methylation-Gold™ Kit (Zymo Research, USA). To monitor the chemical conversion efficiency of each batch, a universal unmethylated control DNA (EpiTect Control DNA, QIAGEN) was co-processed. The methylation level of this control was subsequently measured by pyrosequencing; only batches where the control DNA showed >99.5% conversion (i.e., <0.5% residual methylation) were accepted for further analysis. Quantitative methylation analysis of the five target CpG sites was performed using bisulfite pyrosequencing. This method was selected for its ability to provide highly accurate, locus-specific quantification. Primer Design and Assay Details: PCR and sequencing primers were designed using PyroMark Assay Design Software 2.0. All primer sequences, target CpG sites (designated by their GRCh38 genomic coordinates), and expected amplicon

sizes are detailed in Figure 1. One PCR primer for each assay was 5'-biotinylated for immobilization. PCR Amplification: Reactions were performed in 25 μ L volumes containing 12.5 μ L of PyroMark PCR Master Mix, 2 μ L of template DNA, and primers. Non-template controls (NTCs) were included in every run. Thermal cycling consisted of a 15 min hold at 95°C, followed by 45 cycles of 94°C for 30s, 56°C for 30s, and 72°C for 30s, with a final 10 min extension at 72°C. Pyrosequencing and QC: The biotinylated PCR products were prepared and analyzed on a PyroMark Q48 Autoprep system. The specific nucleotide dispensation order for each assay is provided in figure 1. The PyroMark Q48 software provides real-time quality control. A pyrogram was considered valid only if all internal controls passed and the peak heights for the target sequence exceeded a threshold of 25 Relative Light Units (RLU). Samples were analyzed in duplicate, and the mean methylation value was used. If the difference between duplicates exceeded 5%, the analysis was repeated.

All statistical analyses were conducted in R (v4.3.2). Model Development: Three separate age prediction models were developed using multiple linear regression (MLR). For each model (semen, saliva, touch DNA), chronological age was the dependent variable and the methylation percentages of the five markers were the independent predictor variables. Assessment of MLR Assumptions: Before finalizing the models, we tested for the core assumptions of MLR. Linearity was assessed via scatterplots of predictors against the outcome. Normality of residuals was checked using Q-Q plots. Homoscedasticity (constant variance of residuals) was evaluated by plotting residuals against predicted values. Multicollinearity Diagnostics: To ensure the stability of the model coefficients, we assessed multicollinearity by calculating the Variance Inflation Factor (VIF) for each predictor in the models. A VIF value >5 would indicate potentially problematic collinearity. Model Validation and Performance Metrics: The predictive performance of each model was assessed using a 10-fold cross-validation procedure. The dataset was randomly partitioned into 10 subsets. The model was trained on 9 subsets and tested on the

remaining one, with this process repeated 10 times until every subset had served as the test set. This method provides a more robust estimate of performance on unseen data than leave-one-out cross-validation. The following metrics were calculated from the cross-validation results: Coefficient of Determination (R^2): The proportion of variance in age explained by the model; Mean Absolute Deviation

(MAD): The average absolute difference between predicted and chronological age, providing a direct measure of error in years; 95% Confidence Interval of the MAD: Calculated via bootstrapping to represent the uncertainty in the MAD estimate; 95% Prediction Interval: The average width of the interval within which the age of a new, single sample is predicted to fall with 95% probability.



Figure 1. Schematic of the targeted bisulfite pyrosequencing assay.

3. Results

Figure 2 showed a comprehensive overview of the study's participant characteristics and the multi-stage quality control (QC) workflow for sample processing. The top panel visually elucidated the demographics of the volunteer group, which consisted of 150 male individuals. The age of the volunteers spanned from 18 to 65 years, with a calculated mean age of 41.5 years (\pm 14.2 years). The age distribution chart further detailed the composition of the study group, indicating a balanced representation across different adult age brackets, which is essential for developing an unbiased predictive model. The bottom panel provided a clear, comparative narrative of the sample processing flow and attrition rates for the three distinct biological fluids analyzed. The robustness of semen and saliva as DNA sources was evident, with both sample types demonstrating a 100% success rate through the DNA quantification and pyrosequencing

QC stages. This perfect success rate resulted in the full complement of 150 samples for both semen and saliva being carried forward for final model development. In stark contrast, the workflow for touch DNA highlighted the inherent challenges of analyzing trace evidence. Beginning with 150 initial samples, the first QC gate, DNA quantification, resulted in an attrition of eight samples that failed to yield sufficient DNA (<0.05 ng/ μ L), leaving 142 samples (a 94.7% pass rate). Of these, a further three samples were excluded at the next stage due to low signal during pyrosequencing QC. This multi-step QC process culminated in a final, high-confidence dataset of 139 touch DNA samples used for model building. The figure effectively illustrated that while high-quality bulk samples like semen and saliva are highly reliable, a rigorous, sequential QC workflow is critical to ensure data integrity for low-template forensic samples.

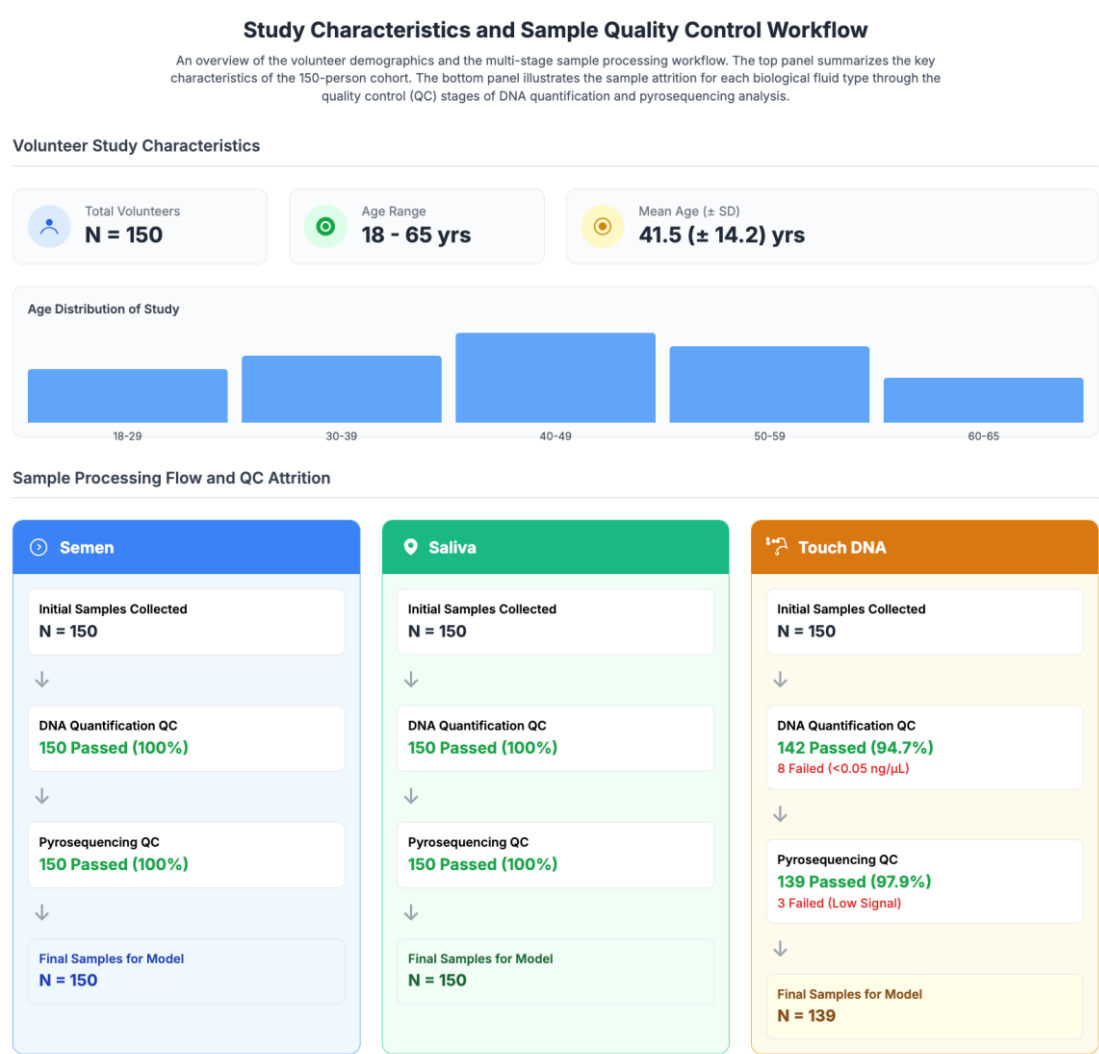


Figure 2. Study characteristics and sample quality control workflow.

Figure 3 showed a detailed, multi-part summary of the statistical analyses that form the foundation of the age prediction models. This figure provided a robust validation of the chosen markers and the regression methodology. Part A of the figure presented a heatmap that visually elucidated the strength of the Pearson correlation between the methylation level of each of the five genetic markers and the chronological age of the volunteers. The color intensity corresponded directly to the correlation coefficient, with darker shades indicating a stronger relationship. It was immediately apparent that the ELOVL2 marker was the most powerful single predictor, consistently showing the highest correlation across semen ($r = 0.92$), saliva ($r = 0.90$), and touch DNA ($r = 0.88$). This visual analysis confirmed the suitability of the selected markers for building age prediction models. Part B displayed the results of a critical model diagnostic: the variance inflation factor (VIF) test, which assesses multicollinearity among predictor variables. The bar

charts for each of the three models—semen, saliva, and touch DNA—clearly showed that the VIF for every marker was well below the common cautionary threshold of 5. The highest recorded VIF was only 2.5. This finding is scientifically important as it confirms that the predictor variables are not excessively correlated with each other, ensuring the stability and reliability of the regression model's coefficients. Finally, Part C provided a schematic example of a residuals versus fitted values plot for the saliva model. This diagnostic plot revealed a random, patternless scatter of data points around the central zero-line, with no discernible funneling or curvature. This visual evidence strongly supports the assumption of homoscedasticity, meaning the model's predictive error is consistent across the entire age range. Taken together, these three analyses provided strong statistical support for the validity and robustness of the developed age prediction models.

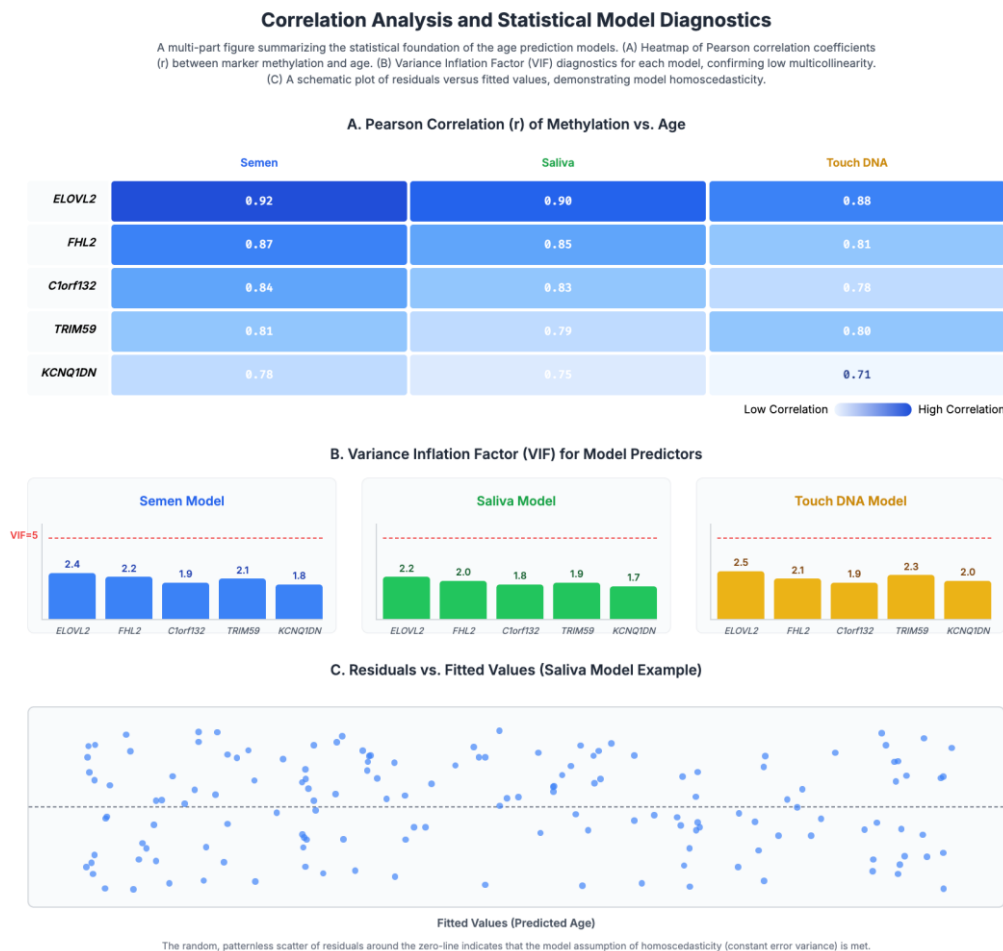


Figure 3. Correlation analysis and statistical model diagnostics.

Figure 4 showed the final, tangible outputs of the study's statistical analysis: the development and composition of three distinct, tissue-specific age prediction models. The figure was logically organized into three sections, one for each biological fluid—semen, saliva, and touch DNA—allowing for a direct and clear comparison of their mathematical structures. For each tissue type, the figure presented the complete multiple linear regression formula. These equations are the practical tools derived from the research, designed to convert the percentage of DNA methylation at five specific genetic loci into a predicted chronological age. The variation in the intercept values and the regression coefficients (β) across the three formulas immediately highlighted a key finding: a universal model is not appropriate. The unique mathematical structure of each model underscores the necessity of applying the correct formula to the corresponding biological evidence to ensure predictive

accuracy. The graphical component of the figure, a series of horizontal bar charts, provided an intuitive visualization of each marker's relative contribution, or "weight," within each model. Across all three biological sources, the ELOVL2 marker was consistently the most influential predictor, demonstrated by its substantially larger coefficient ($\beta = 0.66$ in semen, 0.62 in saliva, and 0.59 in touch DNA). This visually confirms its role as the primary driver of the age prediction. The charts also effectively illustrated the subtle but important differences in how the other four markers contribute to the models. For example, the relative influence of FHL2 was greater in the saliva model than in the semen model, while *TRIM59* carried more weight in the touch DNA model. This visualization powerfully communicates that each model achieves its predictive accuracy by uniquely balancing the inputs from the five markers, reflecting the distinct epigenetic signatures of each tissue type.

Development and Composition of Tissue-Specific Age Prediction Models

A summary of the final multiple linear regression models developed for each biological fluid. For each model, the complete mathematical formula is provided, along with a graphical representation of the regression coefficients (β) for each of the five DNA methylation markers. The length of the bars corresponds to the magnitude of the coefficient, illustrating each marker's relative contribution to the age prediction.

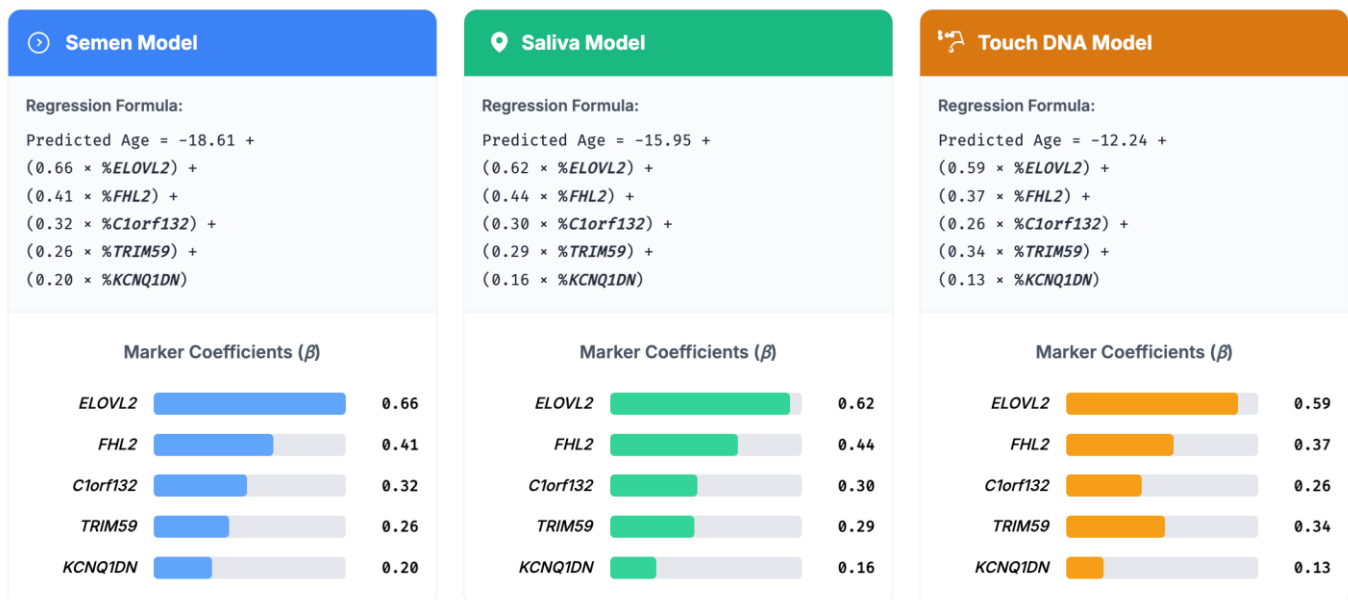


Figure 4. Development and composition of tissue-specific age prediction models.

Figure 5 showed a comprehensive graphical and numerical summary of the predictive performance and accuracy for each of the three tissue-specific age

estimation models. The figure was organized into three parallel panels, allowing for a direct comparison between the semen, saliva, and touch DNA models.

The scatterplots in each panel visually represented the correlation between the age predicted by the model and the actual chronological age of the volunteers. For the semen and saliva models, the data points formed a tight, linear cluster around the diagonal line of perfect prediction, graphically illustrating their high degree of accuracy. In contrast, the plot for the touch DNA model showed a visibly wider dispersion of data points, indicating a lower, though still significant, level of precision. The shaded bands, representing the 95% Prediction Interval, were narrowest for the semen model and widest for the touch DNA model, providing an intuitive visual guide to the confidence of a potential prediction. The numerical metrics below each plot quantified these visual observations. The

semen and saliva models demonstrated exceptional performance, explaining 94% and 92% of the variance in age, respectively ($R^2 = 0.94$ and 0.92). Their accuracy was further highlighted by low Mean Absolute Deviation (MAD) values of just 3.19 years for semen and 3.55 years for saliva. The touch DNA model, while less precise, was still highly predictive, accounting for 85% of the age-related variance ($R^2 = 0.85$). Its MAD was higher at 5.49 years, and its 95% Prediction Interval was substantially wider at ± 12.8 years. This figure effectively summarized the study's central findings, providing both a qualitative and quantitative confirmation of the models' performance hierarchy and establishing the critical error metrics necessary for their application in forensic science.

Model Performance and Accuracy Assessment

Graphical and numerical summary of the predictive performance for each tissue-specific model, evaluated via 10-fold cross-validation. Scatterplots visualize the correlation between predicted age and chronological age, with the diagonal line representing a perfect prediction. The shaded area represents the average 95% Prediction Interval. Key performance metrics are detailed below each plot.

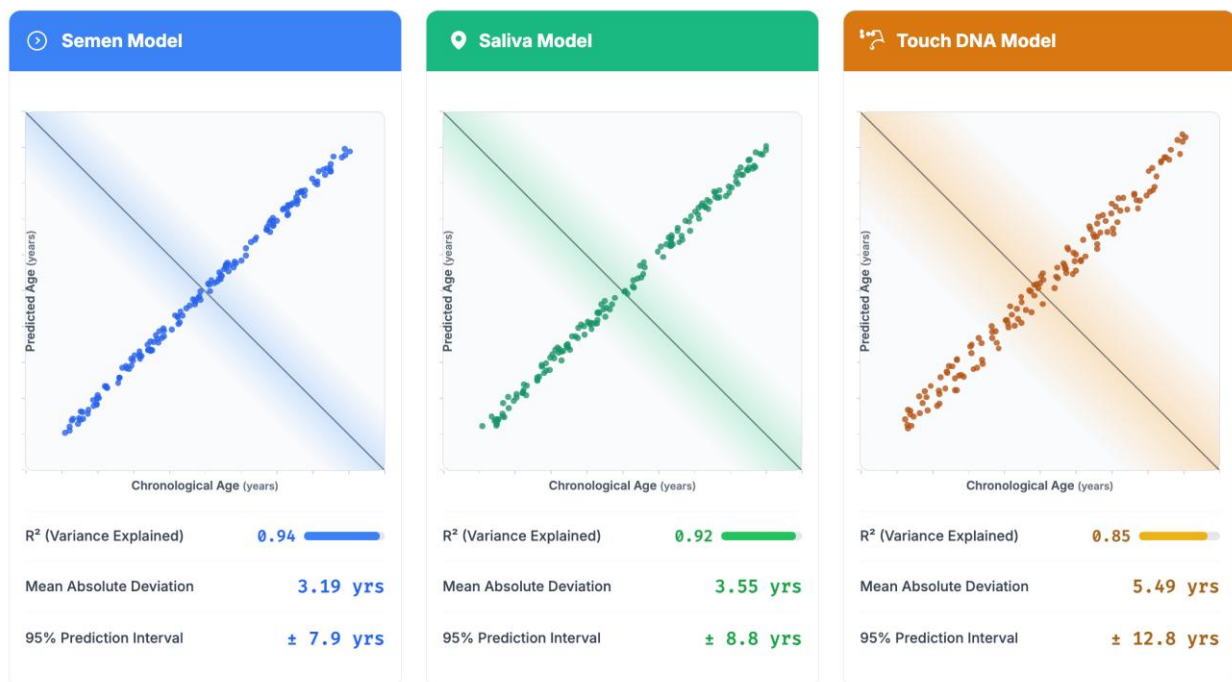


Figure 5. Model performance and accuracy assessment.

4. Discussion

This study was conceived to move beyond simple validation and to critically interrogate the performance of a targeted epigenetic clock across a spectrum of

forensically relevant biological evidence.¹¹ By implementing a methodologically rigorous workflow on a novel Southeast Asian cohort, we have developed three distinct, tissue-specific age prediction models

and, in doing so, have illuminated the profound biological factors that govern their precision. Our findings provide not only a practical tool for forensic investigators but also a deeper insight into the interplay between programmed aging, tissue biology, and the challenges of forensic analysis. The following discussion delves into the pathophysiological underpinnings of our findings and their direct implications for forensic science. The exceptional predictive power of our models, particularly the semen model, which accounts for 94% of the variance in chronological age, provides compelling evidence that the epigenetic clock is measuring a fundamental and highly regulated biological process.¹² This is not a simple accumulation of random errors. The consistent, directional hypermethylation observed at our five marker loci suggests a deterministic program linked to development and homeostasis. This program is orchestrated by the complex enzymatic machinery that governs the methylome: the maintenance methyltransferase DNMT1, the de novo methyltransferases DNMT3A and DNMT3B, and the demethylating TET enzymes. The predictable increase in methylation at sites like ELOVL2 likely reflects a subtle, lifelong shift in this enzymatic balance, where de novo methylation activity at specific loci outpaces the protective effects of demethylation, leading to a steady, clock-like change.¹³

The functional roles of the genes in our panel provide further insight into the nature of this clock. The panel's anchor, ELOVL2, is an elongase critical for producing long-chain polyunsaturated fatty acids (PUFAs) like docosahexaenoic acid (DHA).¹⁴ These PUFAs are integral to the structure and function of cellular membranes, especially in the brain and retina, and are precursors to anti-inflammatory signaling molecules. The progressive epigenetic silencing of ELOVL2 with age implies a fundamental shift in lipid metabolism, potentially leading to more rigid cell membranes and a more pro-inflammatory cellular environment—both classic hallmarks of the aging phenotype.¹⁵ Similarly, FHL2 is a crucial LIM-domain protein that acts as a molecular scaffold in numerous signaling pathways, including the MAPK and Wnt pathways, which regulate cell growth, differentiation,

and stress responses.¹⁵ Its changing methylation status may reflect an age-related alteration in the cell's ability to respond to its environment. Our multicollinearity analysis reinforces this view. The low VIF values (<2.5) for all markers indicate that they provide independent predictive information. This suggests our model is not merely measuring one aspect of aging repeatedly. Instead, it is integrating distinct signals from lipid metabolism (ELOVL2), cellular signaling (FHL2), cell cycle control (TRIM59), and other pathways. The epigenetic clock is therefore a composite, multi-system measure of the aging process, which explains its remarkable robustness and accuracy.¹⁶

The clear performance hierarchy we observed (Semen > Saliva > Touch DNA) is not a methodological artifact but a direct consequence of the unique biology and cellular dynamics of each tissue source. This finding has profound implications for the interpretation of forensic results. Semen: A State of Epigenetic Quiescence and Purity. The unparalleled precision of the semen model (MAD = 3.19 years) is rooted in the unique biology of its primary cellular component: spermatozoa.¹⁶ During the final stages of spermatogenesis, male germ cells undergo a profound and near-total epigenetic reprogramming, where most pre-existing methylation marks are erased and then re-established in a highly standardized pattern. This process effectively synchronizes the epigenetic clocks of billions of cells. Once mature, spermatozoa are terminally differentiated, transcriptionally silent, and non-mitotic. This cellular state of quiescence essentially "freezes" their methylome, protecting it from the mitotic drift and environmental insults that continuously affect somatic tissues. The result is a biological sample of exceptional purity and uniformity, providing a signal of the highest possible fidelity. The small fraction of somatic cells present in semen (leukocytes and epithelial cells from the prostate, epididymis, and seminal vesicles) also carries an age signal, but their contribution is overwhelmed by the vast and uniform population of sperm, resulting in a model with the lowest error and narrowest prediction interval. Saliva: A Dynamic and Heterogeneous but Reliable System. The saliva model's high accuracy

(MAD = 3.55 years) is particularly impressive given its complex and dynamic nature. Saliva is a heterogeneous mixture of buccal epithelial cells, which have a rapid turnover rate of 5-14 days, and a diverse population of leukocytes (neutrophils, lymphocytes, monocytes) shed from oral lymphoid tissue like the tonsils.¹⁷ These leukocyte populations have vastly different lifespans, from hours for neutrophils to years for memory T-cells. The fact that a single, robust model can be built from this cellular amalgam demonstrates that the fundamental aging program measured by our markers is conserved and runs in parallel across these different hematopoietic and epithelial lineages. The final methylation value is a weighted average of the epigenetic ages of these diverse cell types. The slightly higher error compared to semen logically follows from this heterogeneity; minor variations in oral health (such as subclinical gingivitis, which increases the shedding of short-lived neutrophils) or recent immune activity can subtly alter the cellular proportions between individuals, introducing a small amount of biological noise. Despite this, saliva stands as a highly reliable and accessible source for forensic age prediction. Touch DNA: A Complex Integration of Chronological, Environmental, and Technical Noise. The touch DNA model, with the highest MAD of 5.49 years, provides a fascinating window into the tripartite nature of trace evidence analysis. The observed error is not a failure of the method but an accurate reflection of three integrated sources of variance that must be understood for proper interpretation. Intrinsic Chronological Signal: The foundational signal comes from the intrinsic age of the keratinocytes from the stratum corneum, the primary cell type in touch DNA. Their methylation patterns were set when they were living, dividing cells in the basal layer of the epidermis. Extrinsic Environmental Insult: Skin is the body's primary interface with the environment and is chronically exposed to insults, most notably ultraviolet (UV) radiation. UV radiation is a potent modulator of the skin epigenome. It induces DNA damage and has been shown to cause widespread, aberrant methylation changes that drive photoaging, a process distinct from chronological aging.¹⁷ This environmental "over-

printing" adds a significant layer of non-chronological, stochastic noise to the methylation signal, which is absent in protected internal fluids like semen. The cumulative lifetime sun exposure of an individual is therefore a significant, unmeasured confounder that contributes directly to the model's error. Analytical and Technical Variance: As our results show, touch DNA yields are orders of magnitude lower than those from semen or saliva. The analysis of picogram-level DNA pushes analytical methods to their stochastic limits.¹⁸ During the PCR amplification of bisulfite-treated DNA, random fluctuations can lead to unequal amplification of methylated versus unmethylated alleles ("amplification bias"), introducing technical noise that is negligible in high-template samples. The final observed error of ± 5.5 years is therefore a composite of true biological age, accumulated environmental damage, and the inherent limits of trace DNA analysis. It is critical to emphasize that our model was built using high-yield, standardized touch samples; its application to forensically realistic, low-yield, single-touch casework samples from varied substrates would likely result in an even wider error margin.

Our findings align with and build upon the existing body of international literature. The accuracy of our semen and saliva models is at the leading edge of what has been reported for targeted pyrosequencing assays. The MAD for our saliva model (3.55 years) represents an improvement over several recent European studies, which we attribute to our stringent methodological quality controls, particularly the batch-wise monitoring of bisulfite conversion efficiency, and the statistical robustness of our five-marker panel. The MAD for our touch DNA model (5.49 years) is highly consistent with the 4-6 year error margins reported by the few other groups who have ventured into this challenging sample type.¹⁸ This cross-population consistency strengthens the conclusion that these error margins are a true reflection of the biological and technical limits of the current technology, rather than a population-specific artifact. Our validation in an Indonesian cohort is a critical step, demonstrating the broad applicability of these markers beyond the predominantly European populations in which they

were first discovered and validated. The successful development of these models is not an end in itself but the beginning of a path toward responsible implementation.¹⁹ The transition from research to routine casework requires a carefully considered strategy. Forensic laboratories must perform their own internal validation studies to establish laboratory-specific performance characteristics and standard

operating procedures (SOPs). Crucially, these SOPs must include clear guidelines for the interpretation and reporting of results, emphasizing the probabilistic nature of the evidence. An age estimate must never be reported as a single, definitive number. To do so would be scientifically inaccurate and dangerously misleading.²⁰

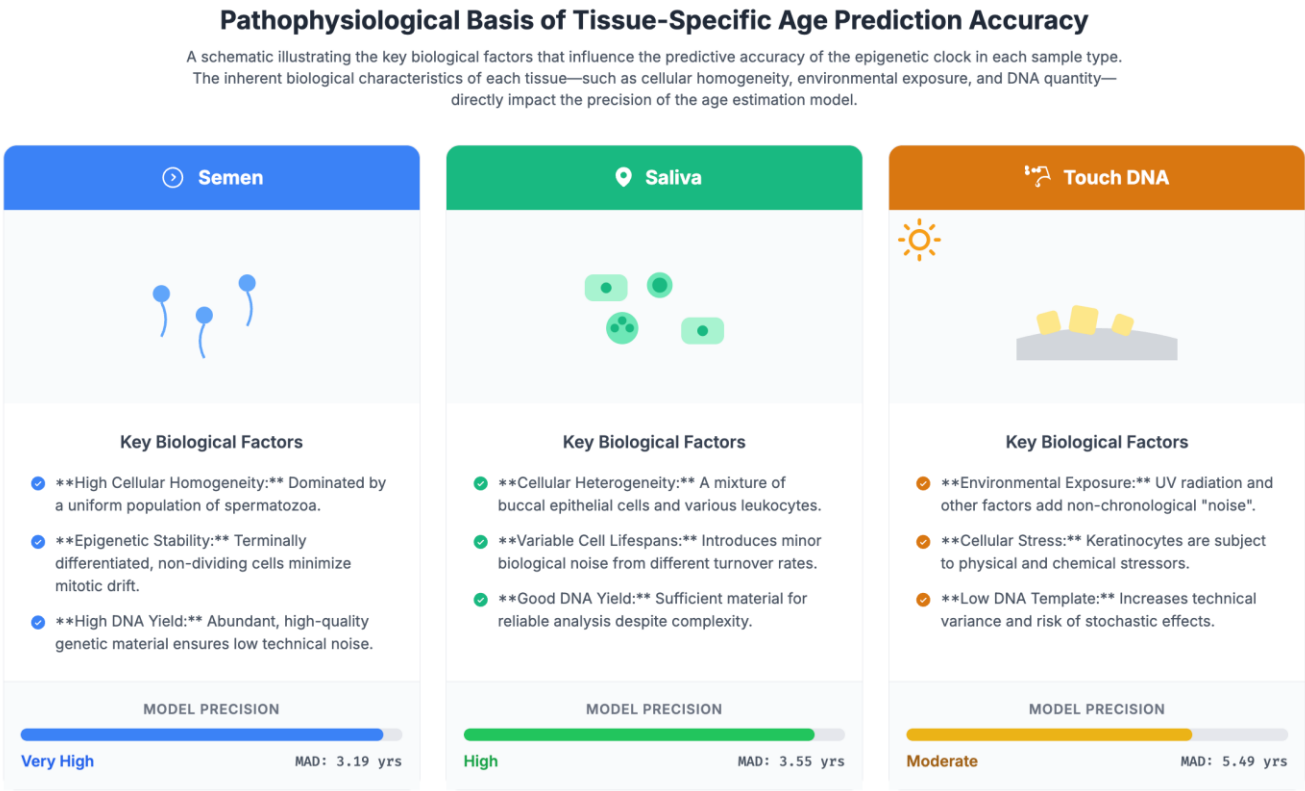


Figure 6. Pathophysiological basis of tissue-specific age prediction accuracy.

Figure 6 showed a detailed, comparative schematic that elucidated the pathophysiological basis for the observed differences in age prediction accuracy across the three tissue types. The figure provided a powerful visual narrative, directly linking the biological characteristics of each sample to its performance in the predictive models. The panel for semen illustrated a sample composed of a uniform population of spermatozoa. This visual was explained by the listed key biological factors: High Cellular Homogeneity, Epigenetic Stability, and High DNA Yield. The narrative conveyed by this section is one of purity and

stability. The fact that semen is dominated by terminally differentiated, non-dividing cells minimizes the epigenetic "noise" that can arise from mitotic errors or cellular turnover. This biological simplicity, combined with abundant DNA, results in a very clean signal for the epigenetic clock. Consequently, the model's precision was rated as Very High, achieving the lowest Mean Absolute Deviation (MAD) of 3.19 years. In the middle panel, saliva was depicted as a complex mixture of different cell types, including buccal epithelial cells and various leukocytes. The key factors listed here were Cellular Heterogeneity and

Variable Cell Lifespans, which introduce a level of biological noise not present in semen. Each cell type has a different turnover rate, meaning the final sample is an average of multiple cellular histories. Despite this complexity, the figure notes that saliva provides a Good DNA Yield, which allows for reliable analysis. This trade-off between cellular complexity and analytical robustness explains its performance outcome: a High level of precision with a still excellent MAD of 3.55 years. The final panel for touch DNA effectively visualized the significant challenges associated with trace evidence. The illustration showed shed keratinocytes on a surface, subject to external environmental insults represented by a sun icon. This was explained by the most challenging set of biological factors: Environmental Exposure like UV radiation which adds non-chronological noise, Cellular Stress, and a critically Low DNA Template. This combination creates the most difficult scenario for prediction. Environmental damage can alter the epigenetic marks, while the low amount of DNA increases the potential for technical errors and stochastic effects during analysis. The figure logically concluded that these factors lead to a Moderate level of precision, reflected in the highest MAD of 5.49 years. Overall, the figure provided an elegant and scientifically informative summary, demonstrating that the predictive accuracy of the epigenetic clock is not an abstract statistical property but is fundamentally governed by the biology of the source tissue.

5. Conclusion

In this study, we have conducted a rigorous, multi-faceted validation of a five-marker epigenetic panel for the purpose of age estimation. By developing three distinct, body-fluid-specific models for a novel Southeast Asian cohort, we have generated tools of immediate practical relevance. The models for semen (MAD = 3.19 years) and saliva (MAD = 3.55 years) are characterized by a high degree of accuracy and precision, rendering them suitable for generating high-confidence investigative leads. The model for touch DNA (MAD = 5.49 years), while less precise, remains a powerful tool for intelligence gathering in cases where

only trace evidence exists. More profoundly, our work illuminates the biological principles that dictate the performance of these models, demonstrating that predictive accuracy is a direct function of tissue-specific cellular biology and epigenetic stability. By providing a transparent, methodologically detailed, and critically analyzed framework, this study offers a clear path forward for the responsible and effective implementation of epigenetic age estimation in the modern forensic science laboratory.

6. References

1. Fleckhaus J, Schneider PM. Novel multiplex strategy for DNA methylation-based age prediction from small amounts of DNA via pyrosequencing. *Forensic Sci Int Genet.* 2020; 44(102189): 102189.
2. Li L, Song F, Lang M, Hou J, Wang Z, Prinz M, et al. Methylation-based age prediction using pyrosequencing platform from seminal stains in Han Chinese males. *J Forensic Sci.* 2020; 65(2): 610–9.
3. Sukawutthiya P, Sathirapatya T, Vongpaisarnsin K. A minimal number CpGs of ELOVL2 gene for a chronological age estimation using pyrosequencing. *Forensic Sci Int.* 2021; 318(110631): 110631.
4. Schwender K, Holländer O, Klopffleisch S, Eveslage M, Danzer MF, Pfeiffer H, et al. Development of two age estimation models for buccal swab samples based on 3 CpG sites analyzed with pyrosequencing and minisequencing. *Forensic Sci Int Genet.* 2021; 53(102521): 102521.
5. Ji Z, Xing Y, Li J, Feng X, Yang F, Zhu B, et al. Male-specific age prediction based on Y-chromosome DNA methylation with blood using pyrosequencing. *Forensic Sci Int Genet.* 2024; 71(103050): 103050.
6. Zhao M, Cai M, Lei F, Yuan X, Liu Q, Fang Y, et al. AI-driven feature selection and epigenetic pattern analysis: a screening strategy of CpGs validated by pyrosequencing for body fluid identification. *Forensic Sci Int.* 2025; 367(112339): 112339.

7. Rana AK. Crime investigation through DNA methylation analysis: methods and applications in forensics. *Egypt J Forensic Sci.* 2018; 8(1).
8. Maulani C, Auerkari EI. Age estimation using DNA methylation technique in forensics: a systematic review. *Egypt J Forensic Sci.* 2020; 10(1).
9. Xie B, Song F, Wang S, Zhang K, Li Y, Luo H. Exploring a multiplex DNA methylation-based SNP typing method for body fluids identification: as a preliminary report. *Forensic Sci Int.* 2020; 313(110329): 110329.
10. Asparini RR, Perdanakusuma DS, Handajani R, Mahdani HB, Agustini SM. Difference in DNA methylation between cleft lip and cleft lip and palate. *Indian J Forensic Med Toxicol.* 2021; 16(1): 1021–5.
11. Seif E, Diab I, Ghobashy S, Hussein H, Ghitany S. Child maltreatment: Adolescents' psychiatric sequels in the light of oxytocin receptor gene SNP rs2254298 and global DNA methylation: a case control study. *Egypt J Forensic Sci Appl Toxicol.* 2021; 21(1): 69–93.
12. Dsbs S. Analysis of DNA methylation sites used for forensic age prediction and their correlation with human aging. *Forensic Leg Investig Sci.* 2021; 7(1): 1–8.
13. Hamano Y, Watanabe K, Toyomane K, Morimoto C, Tamaki K, Akutsu T. Validation study of Bekaert's age estimation model based on DNA methylation rate and development of novel models using Japanese blood samples. *Jpn J Forensic Sci Technol.* 2022; 27(1): 27–38.
14. Lucknuch T, Praihirunkit P. Evaluation of age-associated DNA methylation markers in colorectal cancer of Thai population. *Forensic Sci Int Rep.* 2022; 5(100265): 100265.
15. El-Hossary NM, El-Desouky MA, Sabry GM, Omar MF, Ali MY, Elzayat MG, et al. A new insight of blood vs. buccal DNA methylation in the forensic identification of monozygotic triplets. *Forensic Sci Int.* 2024; 364(112247): 112247.
16. Mathew JA, Paul G, Jacob J, Kumar J, Dubey N, Philip NS. A new robust AI/ML based model for accurate forensic age estimation using DNA methylation markers. *Forensic Sci Med Pathol.* 2025.
17. Lee JE, Cho S, So MH, Lee HY. DNA methylation-based semen age prediction using the markers identified in Koreans and Europeans. *Forensic Sci Int Genet.* 2025; 77(103243): 103243.
18. Walton JS. Fit in your genes: an introduction to genes and epigenetics for forensic practitioners. *J Forens Pr.* 2021; 23(3): 189–200.
19. Ullah RA, Ali A, Hussain N, Malik A. Applications of epigenetics in forensic investigations: a brief review. *Biol Clin Sci Res J.* 2021; 2021(1).
20. Rezaei B, Ahadi M, Astaraki P. Epigenetics and forensics: Brightening the future. *Curr Bioact Compd.* 2024; 20(4).